

# 23-electron octahedral molybdenum cluster complex



*Natalya A. Vorotnikova,<sup>†,‡</sup> Yuri A. Vorotnikov,<sup>†,‡</sup> Igor N. Novozhilov,<sup>†</sup> Mikhail M. Syrovkashin,<sup>†</sup>  
Vladimir A. Nadolinny,<sup>†</sup> Natalia V. Kuratieva,<sup>†,§</sup> David M. Benoit,<sup>||</sup> Yuri V. Mironov,<sup>†,§</sup> Richard I.  
Walton,<sup>⊥</sup> Guy J. Clarkson,<sup>⊥</sup> Noboru Kitamura,<sup>#</sup> Andrew J. Sutherland,<sup>&</sup> Michael A.  
Shestopalov,<sup>\*,†,‡,§</sup> Olga A. Efremova<sup>\*,||</sup>*

*<sup>†</sup>Nikolaev Institute of Inorganic Chemistry SB RAS, 3 Acad. Lavrentiev Ave., 630090  
Novosibirsk, Russian Federation*

*<sup>‡</sup>Scientific Institute of Clinical and Experimental Lymphology – branch of ICG SB RAS, 2  
Timakova str., 630060 Novosibirsk, Russian Federation*

*<sup>§</sup>Novosibirsk State University, 2 Pirogova str., 630090 Novosibirsk, Russian Federation*

*<sup>||</sup>School of Mathematics and Physical Sciences, University of Hull, Cottingham Road, Hull, HU6  
7RX, UK. E-mail: o.efremova@hull.ac.uk*

*<sup>⊥</sup>Department of Chemistry, University of Warwick, Coventry, CV4 7AL*

*<sup>#</sup>Department of Chemistry, Faculty of Science, Hokkaido University, 060-0810 Sapporo, Japan*

*<sup>&</sup>Aston Institute of Materials Research, Aston University, Aston Triangle, Birmingham, B4 7ET,*

*UK*

Molybdenum cluster; Redox; Luminescence; Jahn-Teller distortion; Crystal Structure

**ABSTRACT:** Photoactive transition metal compounds that are prone to reversible redox reactions are important for myriad applications, including catalysis, optoelectronics and sensing. This article describes chemical and electro-chemical methods to prepare cluster complex  $(\text{Bu}_4\text{N})[\{\text{Mo}_6\text{I}_8\}\text{Cl}_6]$ , a rare example of  $23\bar{e}$  cluster complex within the family of octahedral clusters of Mo, W, and Re. The low temperature and room temperature crystal structures, electronic structure and the magnetic, optical and electrochemical properties of this complex are described.

## INTRODUCTION

Systems that demonstrate reversible redox properties combined with photoluminescence properties are highly interesting for applications based on electron transfer or photoinduced electron transfer, such as photovoltaics,<sup>1</sup> photo/electrocatalysis<sup>2, 3</sup> and light-emitting diodes (LEDs).<sup>4-6</sup> In these regards transition metal complexes are in the focus of the global research community, due to the rich diversity of their electrochemical and optical properties. The most famous exemplars of such systems are based on precious metals such as Ru(II) complexes for dye-sensitized solar cells,<sup>1</sup> Re(I) carbonyl complexes for photo-/electro-catalytic reduction of  $\text{CO}_2$ ,<sup>2, 3</sup> and photoluminescent Ir(III) complexes as photoemissive elements of organic LEDs.<sup>4-6</sup>

Photoluminescent octahedral cluster complexes of molybdenum, tungsten and rhenium,  $[\{\text{Mo}_6\text{X}_8\}\text{L}_6]^{2-}$ ,  $[\{\text{W}_6\text{X}_8\}\text{L}_6]^{2-}$  and  $[\{\text{Re}_6\text{Q}_8\}\text{L}_6]^{4-}$  (where X is Cl, Br or I, Q is S, Se or Te and L are apical organic or inorganic ligands), respectively, have recently emerged as a new photoactive elements in photovoltaic<sup>7, 8</sup>, photocatalytic<sup>9-14</sup> and lighting applications.<sup>15, 16</sup> These isoelectronic

cluster complexes have a closed 24 valent electron shell and often demonstrate phosphorescent properties characterised by the emission in the red/near infrared region and long lifetimes (up to 400  $\mu$ s). Moreover, electrochemical studies show that several members of this octahedral cluster family also demonstrate reversible one-electron oxidation that leads to 23-electron complexes.<sup>17-</sup>  
<sup>22</sup> Thus, octahedral metal cluster complexes may be ideal candidates for efficient charge generation and separation.

It should be noted that although cyclic voltammetry data have been reported for many octahedral cluster complexes, only a few examples of 23-electron cluster complexes have been isolated as a single phase. These include  $[\{\text{Re}_6\text{Q}_8\}(\text{CN})_6]^{3-}$  (Q = S, Se, Te) and  $[\{\text{Re}_6\text{Q}_8\}\text{Y}_6]^{3-}$  (Q = S, Se; Y = Cl, Br, I) compounds synthesised by chemical or electrochemical oxidation of the corresponding 24-electron parent cluster precursors<sup>20, 23-29</sup> examples of a 23 $\bar{e}$  tungsten cluster compounds, containing  $[\{\text{W}_6\text{X}_8\}\text{X}_6]^-$  (X=Br, I)<sup>30-37</sup>. In regards to the molybdenum cluster complexes compounds containing cluster anions  $[\{\text{Mo}_6\text{X}_8\}\text{Y}_6]^{2-}$  (where X is an inner halogen ligand and Y is an outer organic or inorganic ligand) are well known and have been extensively studied for the last half century, especially those based on  $[\{\text{Mo}_6\text{Cl}_8\}\text{Cl}_6]$ .<sup>2-7, 38-48</sup> In previous works<sup>22, 46</sup> it has been shown that complexes  $[\{\text{Mo}_6\text{X}_8\}\text{Y}_6]^{2-}$  undergo quasi-reversible one-electron oxidation when X = Y = Cl or Br and irreversible oxidation, when X = Y = I. Moreover, Gray et al. succeeded in generation of  $[\{\text{Mo}_6\text{Cl}_8\}\text{Cl}_6]^-$  in solution upon potentiostatic electrolysis, and noted that the ion is not stable in solution over time.<sup>39</sup> Works of Nocera et al. and Gray et al. also suggest that  $[\{\text{Mo}_6\text{Cl}_8\}\text{Cl}_6]^-$  generated *in situ* can act as a very strong oxydising agent.<sup>39, 49</sup> Despite this prior work, to the best of our knowledge, the corresponding halide compounds containing 23 electrons or indeed any molybdenum cluster complexes with the fully halide core  $\{\text{Mo}_6\text{X}_8\}^-$  (X=Cl, Br, I) has not been isolated and characterised as a single phase previously.

In this article we present the synthesis and physico-chemical and electronic properties of the first example of a stable 23 $\bar{e}$  octahedral molybdenum cluster complex  $(\text{Bu}_4\text{N})[\{\text{Mo}_6\text{I}_8\}\text{Cl}_6]$  and detailed study of the 23 $\bar{e}$ /24 $\bar{e}$  system  $[\{\text{Mo}_6\text{I}_8\}\text{Cl}_6]^{-2-}$ .

## EXPERIMENTAL SECTION

### Materials

$(\text{Bu}_4\text{N})_2[\{\text{Mo}_6\text{I}_8\}(\text{NO}_3)_6]$  was synthesised according to previously reported procedures.<sup>50</sup> All other reactants and solvents were purchased from Fisher, Alfa Aesar or Sigma-Aldrich and used as received.

### Instrumentation

Elemental analyses were obtained using a EuroVector EA3000 Elemental Analyser. Energy-dispersive X-ray spectroscopy (EDS) was performed on a Hitachi TM3000 TableTop SEM with Bruker QUANTAX 70 EDS equipment; results are reported as the ratio of the heavy elements: Mo, I, and Cl; the relative error of the method is about 5%. FTIR spectra were recorded on a Bruker Vertex 80 as KBr disks. X-Ray powder diffraction patterns were recorded on a Philips APD 1700 instrument with  $\lambda_{\text{Cu}}(\text{K}_{\alpha 1}, \text{K}_{\alpha 2}) = 1.54059, 1.54439 \text{ \AA}$ . The thermal properties were studied on a Thermo Microbalance TG 209 F1 Iris (NETZSCH) in the temperature range 25–850 °C with a heating rate of 10°/min in a helium flow (30 mL/min). Optical diffuse reflectance spectra were measured at room temperature on a Shimadzu UV-Vis-NIR 3101 PC spectrophotometer equipped with an integrating sphere and reproduced in the form of Kubelka–Munk theory. The DSC measurements were carried out on a differential scanning calorimeter Netzsch DSC 204F1 Phoenix. The heating rate was 6 K/min and argon flow was 25 mL/min.

The mass spectrometric (MS) detection was performed on an electrospray ionization quadrupole time-of-flight (ESI-q-TOF) high-resolution mass spectrometer Maxis 4G (Bruker Daltonics, Germany). The MS calibration was performed with ESI-L calibration mix (Agilent, USA).

### **Synthesis of $(\text{Bu}_4\text{N})_2[\{\text{Mo}_6\text{I}_8\}\text{Cl}_6](1)$**

2 mL of 38% hydrochloric acid (25 mmol, 10 eq.) was added to 100 mL solution of  $(\text{Bu}_4\text{N})_2[\{\text{Mo}_6\text{I}_8\}(\text{NO}_3)_6]$  (1 g, 0.41 mmol) in acetone and the reaction mixture was stirred for 1 h. The volume of the solvent was then reduced to 3 mL using a rotary evaporator. This resulted in the formation of orange needle-like crystals of the product. The crystals were collected by filtration and washed in situ on the filter paper with an excess of water until the filtrate was colorless and had neutral pH. Yield: 704.7 mg (77 %). ESI-MS (-): 902.2224 ( $[\{\text{Mo}_6\text{I}_8\}\text{Cl}_6]^{2-}$ ); 2046.7377 ( $(\text{Bu}_4\text{N})[\{\text{Mo}_6\text{I}_8\}\text{Cl}_6]^-$ ). For  $\text{C}_{32}\text{H}_{72}\text{NMo}_6\text{I}_8\text{Cl}_6$  found: C 16.1 %, H 3.0 %, N 1.3 %.; calculated: C 16.8%, H 3.2%, N 1.2%. EDS: Mo:I:Cl = 6.0:7.7:5.8.

### **Synthesis of $(\text{Bu}_4\text{N})[\{\text{Mo}_6\text{I}_8\}\text{Cl}_6](2)$**

#### **Method 1 - Chemical oxidation (2a)**

0.5 mL (8.2 mmol) of concentrated  $\text{HNO}_3$  was added to 50 mL chloroform solution of **1** (100 mg, 0.04 mmol). The obtained mixture was stood for two days. The dark-green powder formed was isolated by centrifugation and washed with an excess of water by cycles of resuspension, centrifugation and decantation. Yield: 80.5 mg (90%). For  $\text{C}_{16}\text{H}_{36}\text{NMo}_6\text{I}_8\text{Cl}_6$  found: C 8.4%, H 1.7%, N 0.7%; calculated: C 9.4%, H 1.8%, N 0.7%. EDS: Mo:I:Cl = 6.1:7.8:5.8.

#### **Method 2- Electro-precipitation (2b)**

Electro-precipitation was conducted using a VA 797 Computrace (Metrohm) voltammetric instrument. A platinum rod (L15×Ø2 mm) was used as the working electrode. Compound **1** (80 mg, 0.035 mmol) was dissolved in acetone (10 mL) and placed into an electrochemical cell. Dark-

green crystals of compound **2** were then grown on the anode by applying a constant potential of +1.5 V (rel. AgCl/Ag) for 12 hours at room temperature with constant stirring. The crystals grown on the electrode were carefully collected using a spatula and dried. The current varied within a diapason of 100-400  $\mu$ A. Yield: 55 mg (77 %). For  $C_{16}H_{36}NMo_6I_8Cl_6$  found: C 9.3 %, H 1.7 %, N 0.7 %.; calculated: C 9.4%, H 1.8%, N 0.7%. EDS: Mo:I:Cl = 6:7.7:5.3.

### Crystal structure determination

Diffraction data for compound **1** we collected at 290 and 150 K on an automated Agilent Xcalibur diffractometer equipped with an area AtlasS2 detector (graphite monochromator,  $\lambda(\text{MoK}\alpha) = 0.71073 \text{ \AA}$ ,  $\omega$ -scans). Integration, absorption correction, and determination of unit cell parameters were performed using the CrysAlisPro program package.<sup>51</sup> The structures were solved by dual space algorithm (SHELXT<sup>52</sup> and refined by the full-matrix least squares technique (SHELXL<sup>53</sup>).

Single-crystal X-ray diffraction data for **2** were recorded for different samples:

**2a** – crystals were grown in an aged chloroform solution containing  $(\text{Bu}_4\text{N})_2[\{\text{Mo}_6\text{I}_8\}(\text{NO}_3)_6]$ : the data were collected on an Oxford Diffraction Gemini four-circle system with a Ruby CCD area detector fitted with graphite monochromatised  $\text{MoK}\alpha$  radiation ( $\lambda = 0.71073 \text{ \AA}$ ). The crystal was held at 298(2) K with the Oxford Cryosystem, Cryostream Cobra. **2b** – crystals obtained by electro-precipitation: the data were collected at 298 and 150 K on a Bruker Nonius X8Apex 4K CCD diffractometer fitted with graphite monochromatised  $\text{MoK}\alpha$  radiation ( $\lambda = 0.71073 \text{ \AA}$ ). All crystallographic information is summarised in Table S1. Absorption corrections were made empirically using the SADABS program.<sup>54</sup> The structures were solved by the direct method and further refined by the full-matrix least-squares method using the SHELXTL program package.<sup>54</sup> All non-hydrogen atoms were refined anisotropically. The positions of the hydrogen atoms of the

tetra-n-butylammonium cation were calculated corresponding to their geometrical conditions and refined using the riding model with freely rotating methyl groups. Two of the butyl chains of the  $\text{Bu}_4\text{N}^+$  in **2a** and **2b** (T = 298 K) were modelled as disordered. One chain in **2a** was refined over two positions and refined to an occupancy of 80:20 (C14-C17 to C14A-C17A). The disorder of the other chain was refined by fixing the occupancy of the two disordered chains at 75:25 (C10-C13:C10A-C13A). The disorder of the other chain was refined by fixing the occupancy of the two disordered chains at 75:25 (C10-C13:C10A-C13A). Also both disordered chains in **2b** (T = 298 K) were refined over two positions and refined with free variable occupancy factors of 69:31 (C31A-C34A:C31B-C34B) and 78:22 (C41A-C44A:C41B-C44B). Several SIMU, DELU, ISOR and DFIX restraints were used to give these disordered components chemically sensible bond lengths, angles and thermal parameters.

CCDC 1425980, 1576975-1576976 and 1588848-1588849 contain the supplementary crystallographic data for this paper. These data can be obtained free of charge from the Cambridge Crystallographic Data Centre ([www.ccdc.cam.ac.uk/data\\_request/cif](http://www.ccdc.cam.ac.uk/data_request/cif)).

### **Cyclic voltammetry**

Cyclic voltammetry (CV) of **1** (1,3 mM) was performed using a Metrohm 797 VA Computrace instrument in 10 cm<sup>3</sup> electrochemical cell equipped with a glassy carbon electrode (working area - 3 mm<sup>2</sup>) as the working electrode, saturated silver / silver chloride (Ag/AgCl) in 3M KCl as a reference electrode and a platinum rod as a counter electrode. A 0.15 M solution of tetra-n-butylammonium perchlorate ( $\text{Bu}_4\text{NClO}_4$ ) in acetone was used as the electrolyte in which 1-2 mM of **1** was dissolved. The solutions were degassed by purging with argon for at least 5 minutes prior to recording the CV measurements.

### **Magnetic properties characterization**

EPR analysis was undertaken at room temperature on an E109 spectrometer (Varian) at 9.5GHz. The electrochemical oxidation of **1** was undertaken directly inside of the resonator of the spectrometer. An acetone solution of **1** was placed into a flat tube with a platinum net electrode and oxidised at a potential of 1.5V. 2,2-Diphenyl-1-picrylhydrazyl ( $g = 2.0036$ ) was used to calibrate the field in the EPR spectrometer. The temperature dependence of the magnetic susceptibility was measured by the Faraday method at 7.3 kOe over the temperature range 80–300-80 K. During the measurements the sample were placed in helium atmosphere at 10 Torr pressure. The temperature stabilization was controlled by pid-regulator Delta DTB9696. The data were recorded using quartz torque microbalance and precision digital voltmeter Keysight 34465A.

### **Photoluminescence Measurements**

For photoluminescence measurements, powdered samples of the complexes were placed between two non-fluorescent glass plates. The absorbance of a blank acetone solution was set at  $< 0.1$  at 355 nm. The solutions were poured into quartz cuvettes. To deaerate, the solution was purged with an Ar-gas stream for 30 min and then the cuvettes were sealed. Measurements were carried out at 298 K. The samples were excited by 355-nm laser pulses (6 ns duration, LOTIS TII, LS-2137/3). Corrected emission spectra were recorded on a red-light-sensitive multichannel photodetector (Hamamatsu Photonics, PMA-11). For emission decay measurements, the emission was analysed using a streakscope system (Hamamatsu Photonics, C4334 and C5094). The emission quantum yields were determined using an Absolute Photo-Luminescence Quantum Yield Measurement System (Hamamatsu Photonics, C9920-03), which comprised a xenon excitation light source (the excitation wavelength was set at 400 nm), an integrating sphere, and a red-sensitive multichannel photodetector (Hamamatsu Photonics, PMA-12).

### **DFT calculations**

Each compound was fully optimised **without imposing any symmetry point group** in its low-spin state at the B3LYP-D3BJ level of theory,<sup>55-57</sup> along with a def2-TZVPP basis set<sup>58</sup> and a def2-TZVPP/J auxiliary basis set,<sup>59</sup> using the ORCA 4.0.1 suite of programs.<sup>60</sup> Note that the def2 basis set uses pseudo potentials for Mo, and I to remove core electrons and the RIJ-COSX approximation was used to accelerate calculations.<sup>61</sup>

## RESULTS AND DISCUSSION

### Synthesis

In this work we present the chemical and electrochemical synthesis and isolation of the first 23e molybdenum cluster complex  $(\text{Bu}_4\text{N})[\{\text{Mo}_6\text{I}_8\}\text{Cl}_6]$  (**2**). Serendipitously, this compound was first obtained as a few dark green crystals formed in an aged  $\text{CHCl}_3$  solution of cluster compound  $(\text{Bu}_4\text{N})_2[\{\text{Mo}_6\text{I}_8\}(\text{NO}_3)_6]$ . Single crystal X-ray analysis confirmed the composition of these crystals to be  $(\text{Bu}_4\text{N})[\{\text{Mo}_6\text{I}_8\}\text{Cl}_6]$ . It is well-known that  $(\text{Bu}_4\text{N})_2[\{\text{Mo}_6\text{I}_8\}(\text{NO}_3)_6]$  is a highly labile complex,<sup>47, 62-64</sup> while it is also well-known that during prolonged storage in the presence of light and oxygen, chloroform converts slowly to phosgene ( $\text{COCl}_2$ , **Warning: Highly poisonous, if inhaled!**), releasing  $\text{HCl}$ .<sup>65</sup> **Thus, there are two processes that take place in the solution of  $(\text{Bu}_4\text{N})_2[\{\text{Mo}_6\text{I}_8\}(\text{NO}_3)_6]$  in chloroform: the oxidation of the cluster core and the replacement of the  $\text{NO}_3^-$  ligands by  $\text{Cl}^-$ . Attempts to oxidise freshly prepared  $(\text{Bu}_4\text{N})_2[\{\text{Mo}_6\text{I}_8\}(\text{NO}_3)_6]$  in chloroform electrochemically showed that this compound is not electrochemically active in the diapason -1.8 – 2.3 V (vs.  $\text{AgCl}/\text{Ag}$ ). On the other hand as we demonstrate below that  $[\{\text{Mo}_6\text{I}_8\}\text{Cl}_6]^{2-}$  does oxidise reversibly both chemically (by nitric acid) and electrochemically.** It can therefore be suggested that the formation of  $[\{\text{Mo}_6\text{I}_8\}\text{Cl}_6]^-$  from  $[\{\text{Mo}_6\text{I}_8\}(\text{NO}_3)_6]^{2-}$  in chloroform is a two-step process, in which complex  $[\{\text{Mo}_6\text{I}_8\}\text{Cl}_6]^{2-}$  was first formed from

$[\{\text{Mo}_6\text{I}_8\}(\text{NO}_3)_6]^{2-}$  as a result of the terminal ligand substitution, which was then oxidised by the released nitric acid (Scheme 1).



**Scheme 1** Equation showing the two-step generation of  $[\{\text{Mo}_6\text{I}_8\}\text{Cl}_6]^-$  from  $[\{\text{Mo}_6\text{I}_8\}(\text{NO}_3)_6]^{2-}$ .

To test this hypothesis we subsequently synthesised  $(\text{Bu}_4\text{N})_2[\{\text{Mo}_6\text{I}_8\}\text{Cl}_6]$  (**1**) by the direct reaction of a  $(\text{Bu}_4\text{N})_2[\{\text{Mo}_6\text{I}_8\}(\text{NO}_3)_6]$  acetone solution with hydrochloric acid. Although our method of synthesising compound **1** is different to one reported earlier by Bruckner,<sup>66</sup> energy-dispersive X-ray spectroscopy, mass-spectroscopy (Figure S1) and elemental analysis confirm that compound **1** is indeed the same material as that reported earlier. The reaction of **1** with an aqueous solution of  $\text{HNO}_3$  did indeed produce  $(\text{Bu}_4\text{N})[\{\text{Mo}_6\text{I}_8\}\text{Cl}_6]$  (**2a**) in the form of a green powder.

The redox properties of halide molybdenum cluster complexes  $[\{\text{Mo}_6\text{X}_8\}\text{X}_6]^{2-}$  ( $\text{X} = \text{Cl}, \text{Br}, \text{I}$ ) have been studied before by several groups, including ours.<sup>22, 46</sup> These studies demonstrated that chloro- and bromo- ions undergo one-electron quasi-reversible oxidation in the positive potential region, while  $[\{\text{Mo}_6\text{I}_8\}\text{I}_6]^{2-}$  oxidizes irreversibly.<sup>22, 46</sup> Moreover, the potentials of oxidation decrease with increase in the atomic number of the halogen atom. The study of mixed halide compound **1** by cyclic voltammetry in the region potential 0 – 1.5 V also reveals a quasi-reversible oxidation potential  $E_{1/2} = 1.26$  V (Figure 1). The oxidation and reduction currents have a linear dependence upon  $\sqrt{\nu}$ , where  $\nu$  is the scan rate, which is in agreement with Randles–Sevcik equation and signifies that electron transfer is dependent solely on the diffusion rates to the electrodes (Figure S2).

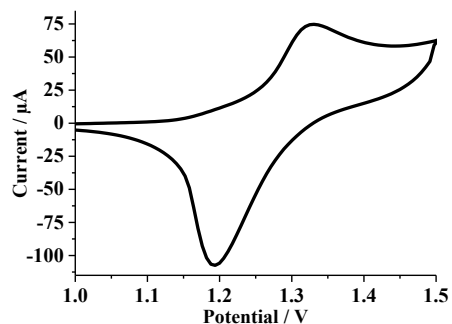


**Figure 1.** Cyclic voltammogram of compound **1** vs Ag/AgCl in 3M KCl reference electrode.

Based on the above CV data, **2** was also obtained by electrochemical oxidation of **1** in an electrochemical cell at a constant potential of 1.5 V on a platinum electrode (**2b**) (Figure. 2). Elemental analysis data of the powders, generated by both chemical and electrochemical methods, were very similar and consistent with the theoretical composition for  $(\text{Bu}_4\text{N})[\{\text{Mo}_6\text{I}_8\}\text{Cl}_6]$ . Moreover, the powder XRD data of products generated by both oxidation methods corresponded to the diffractogram generated from single crystal X-ray structure (Figure S3).



**Figure 2.** Photograph of a platinum rod electrode covered with crystals of compound **2b**.

Notably, while precursor **1** is readily soluble in different organic solvents, such as acetone, acetonitrile, dichloromethane, dimethyl sulfoxide, tetrahydrofuran, *N,N*-dimethylformamide, compound **2** dissolves well only in dimethyl sulfoxide and dimethylformamide and slowly in acetone producing an orange-green or orange solution, which suggests that  $[\{\text{Mo}_6\text{I}_8\}\text{Cl}_6]^-$  is slowly reduced back to  $[\{\text{Mo}_6\text{I}_8\}\text{Cl}_6]^{2-}$  by these mildly reducing solvents (Figure 3). In order to prove the possibility of chemical reduction we used a classical reducing agent, hydrazine hydrate and achieved an efficient reduction of  $[\{\text{Mo}_6\text{I}_8\}\text{Cl}_6]^-$ . When a small amount of acetone followed by hydrazine hydrate was added to **2**, the evolution of nitrogen gas was observed. After 30 s the reaction stopped and the green powder had completely dissolved producing a yellow/brown solution that luminesced brightly and gave similar absorption spectra to those obtained for compound **1**. (Figure 4). Thus the oxidation of **1** is also a chemically-reversible process.

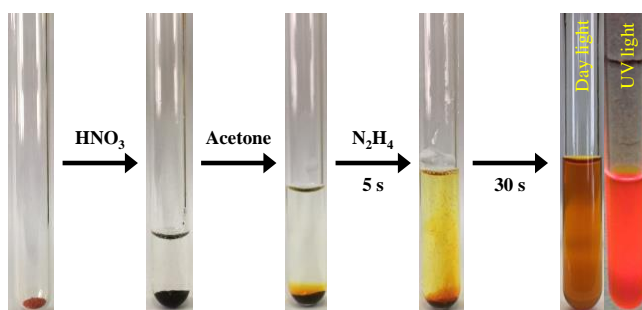


**Figure 3.** Test-tube reactions that illustrate the redox properties of compounds **1** and **2**.

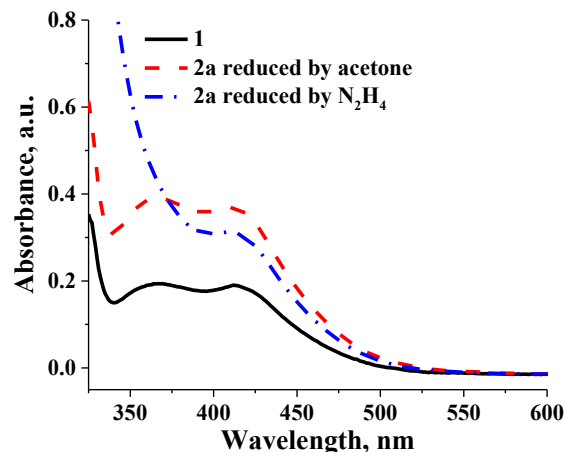


**Figure 4.** UV-vis Absorbance spectra of **1** and **2a** after reduction with acetone (slowly) and  $\text{N}_2\text{H}_4$  (fast). The pronounced shoulder below 370 nm in the latter case is due to the excess of hydrazine.

### Characterisation of 23-electron compound **2**

#### Crystal structure of **2**.

Both crystals obtained by chemical oxidation (**2a**) and electrochemical oxidation (**2b**) were characterised by single crystal and powder diffraction analysis. The crystal structure data of **2b** were also recorded at two different temperatures: 298 K and 150 K. The details of these experiments are summarised in Table 1S. All three crystal data sets gave an identical crystal structure that belongs to the triclinic space group,  $P\bar{1}$ , and contains two halves of two cluster anions  $[\{\text{Mo}_6\text{I}_8\}\text{Cl}_6]^-$  and a  $\text{Bu}_4\text{N}^+$  cation in an asymmetric unit cell. The structure of the cluster anion  $[\{\text{Mo}_6\text{I}_8\}\text{Cl}_6]^-$  is similar to that of other octahedral cluster complexes (Figure S4). Specifically, the anion consists of a  $\text{Mo}_6$  octahedron, the triangular faces of which are coordinated by iodide ligands in a  $\mu_3$ -mode. Each molybdenum atom is additionally coordinated by terminal chloride ligands. The centres of the cluster anions lie on an inversion centre with special positions.

There are therefore two crystallographically independent, but chemically identical cluster anions and two crystallographically identical  $\text{Bu}_4\text{N}^+$  cations per unit cell (Figure 5).

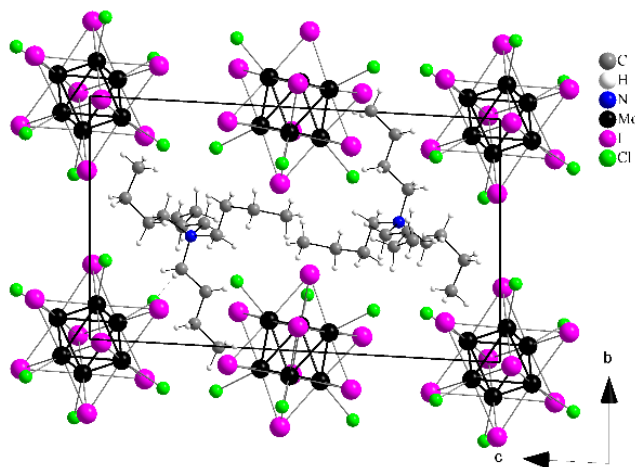


**Figure 5.** Structure of  $(\text{Bu}_4\text{N})[\{\text{Mo}_6\text{I}_8\}\text{Cl}_6]$ .

Table 1 summarises the Mo–Mo, Mo–I and Mo–Cl bond lengths for both **1** and **2**. These data demonstrate that oxidation of the cluster anion does not affect the length of Mo–I and Mo–Cl, but leads to slight elongation of the Mo–Mo bonds. This, in agreement with a number of previous reports, indicates that the HOMO orbital of the molybdenum clusters, which is bonding in nature, has significant input from the molybdenum orbitals.<sup>67-69</sup>

**Table 1.** Bond lengths Mo–Mo, Mo–I and Mo–Cl for **1** and **2**.

	<b>1</b> <sup>66</sup>	<b>1</b>	<b>1</b>	<b>2a</b>	<b>2b</b>	<b>2b</b>
	RT	290 K	150 K	298 K	150 K	298 K
Mo-I	2.775(2)	2.773(3)- 2.789(3)	2.7734(4)- 2.7970(4)	2.7688(8)- 2.8091(7)	2.758(2)- 2.791(2)	2.762(2)- 2.789(2)
Mo-Cl	2.460(6)	2.442(7)- 2.474(8)	2.4749(9)- 2.4800(9)	2.440(2)- 2.461(2)	2.429(4)- 2.448(3)	2.434(5)- 2.448(4)

Mo-Mo	2.655(2)	2.675(3)- 2.696(3)	2.6746(4)- 2.6825(4)	2.6838(7)- 2.7258(8)	2.672(2)- 2.709(2)	2.677(2)- 2.704(2)
-------	----------	-----------------------	-------------------------	-------------------------	-----------------------	-----------------------

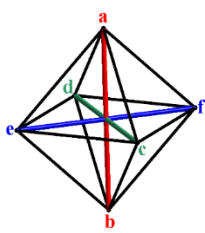
### Jahn-Teller distortion

In the earlier studies of  $23\bar{e}$  rhenium cluster complexes it was shown that these highly symmetric complexes ( $O_h$  point group) undergo Jahn-Teller distortion.<sup>25, 70, 71</sup> Jahn-Teller distortion was also suggested for  $[\{Mo_6Cl_8\}Cl_6]^-$  on the bases of the EPR study of electrochemically generated ions in frozen solution.<sup>39</sup> In contrary, for  $[\{W_6Br_8\}Br_6]^-$  – neither EPR nor single crystal XRD of the  $(Ph_3P)_2N^+$  salt shown Jahn-Teller distortion.<sup>34</sup> To evaluate whether the cluster in the compound **2** undergoes Jahn-Teller distortion or not, the structures of  $Mo_6$  octahedra in **2b** determined at 150 K and 298 K were compared with those of compound **1**. Table 2 summarises the distances between opposite vertices in  $Mo_6$  octahedra in both compounds. It can be seen that the cluster in compound **1** is an almost perfect octahedron and the difference between the largest and the smallest distance being maximum 0.018 Å at room temperature and even smaller (0.006 Å) at 150 K. The distortion of the oxidised  $Mo_6$  octahedron has an opposite dependence on the temperature and for the two crystallographically independent clusters the difference between the largest and smallest distances is 0.008 Å and 0.023 Å at 298 K and 0.032 Å and 0.050 Å at 150 K. Notably as well that at lower temperature these distances in case of compound in average are also somewhat shorter than the corresponding in the oxidised cluster in particular at low temperature 3.787 Å and 3.805 Å, for **1** and **2** respectively. Once again, this observation signifies destabilisation of the  $23\bar{e}$  cluster in comparison with  $24\bar{e}$  one.

Lowering temperature thus noticeably increases distortion, which is convincing evidence of the dynamic Jahn-Teller distortion. Interestingly, in compound **2** two independent  $Mo_6$  clusters

undergo different modes of  $D_{4h}$  distortion upon cooling: one cluster contracts, while another one elongates along an  $h$  axis (Figure 6).

**Table 2.** The distances between opposite vertexes in **1** at RT, 290 and 150 K and **2b** at 298 and 150 K.

	Vertex	<b>2b</b> , 1 <sup>st</sup> octahedron		<b>2b</b> , 2 <sup>nd</sup> octahedron		<b>1</b> <sup>66</sup>	<b>1</b>	<b>1</b>
		298 K	150 K	298 K	150 K	RT*	290 K	150 K
	<b>a-b</b>	3.7921(2)	3.7754(1)	3.8035(2)	3.8210(2)	3.7711(2)	3.8111(3)	3.7838(5)
	<b>c-d</b>	3.8123(2)	3.8222(2)	3.8088(2)	3.8052(2)	3.7644(2)	3.7964(3)	3.7894(5)
	<b>e-f</b>	3.8154(2)	3.8257(2)	3.8004(2)	3.7892(2)	3.7695(2)	3.7928(3)	3.7885(4)

\*RT – room temperature

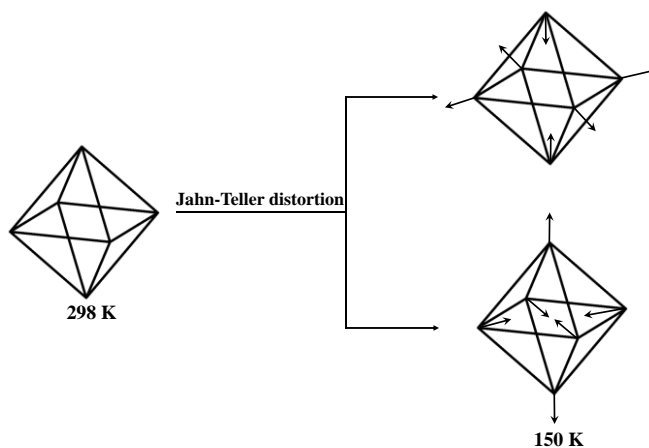


**Figure 6.** The  $D_{4h}$  distortion modes of  $23 \bar{e}$   $\text{Mo}_6$  octahedron in the structure of **2b** upon cooling.

In order to understand the origins of the observed Jahn-Teller distortion in compound **2**, we performed density functional theory calculations of cluster anions  $[\{\text{Mo}_6\text{I}_8\}\text{Cl}_6]^{2-}$  and  $[\{\text{Mo}_6\text{I}_8\}\text{Cl}_6]^-$  to determine their electronic structures at their optimal geometries. The results are summarised in Figure 7, which shows the energy of selected levels around the highest occupied

molecular orbitals (HOMOs). One can see that the last five occupied orbitals of the 24-electron anion exhibit complementary symmetry and are all energetically near-degenerate. This is indicative of a high-symmetry combination of the Mo d orbital with involvement of the Cl p orbitals in a bonding combination. The electronic structure of the 23-electron anion is very different: we note that there is an energetic difference between the alpha (spin up) and beta (spin down) orbitals of the last 5 (4) occupied orbitals. This anion shows significant asymmetry, with a single Mo atom interacting with the iodine atoms (lowest depicted alpha orbital, antibonding interaction). The SOMO is markedly asymmetric due to the uneven electronic occupation. This causes a visible geometric distortion of the cluster, *i.e.* Jahn-Teller distortion. Indeed the calculated distances for the 24-e cluster are  $a-b = c-d = e-f = 3.763 \text{ \AA}$  and for the 23-e cluster are  $a-b = 3.911 \text{ \AA}$ ,  $c-d = 3.732 \text{ \AA}$  and  $e-f = 3.731 \text{ \AA}$ , *i.e.* suggesting  $D_{4h}$  distortion type. The appearance in the crystal structure of two different types of distortion are likely the result of packing effects that are not taken into account in our calculations in vacuum.

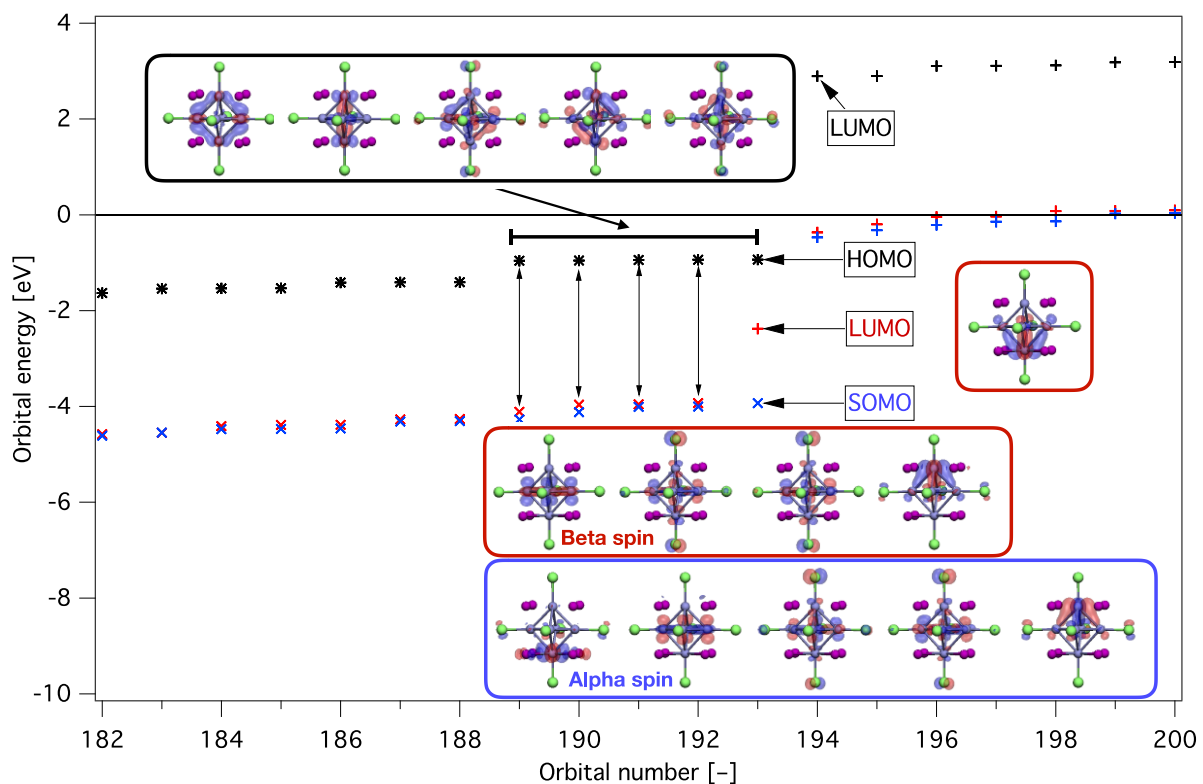


**Figure 7.** Electronic energy levels for compound **1** (black asterisks) and **2** (blue crosses, alpha (up) spin and red crosses, beta (down) spin). Unoccupied orbitals are represented as (+), black for compound **1** and blue/red for alpha/beta spin orbitals of compound **2**. The last 5 occupied molecular orbitals are depicted for each compound using a 0.05  $\bar{e}$ /bohrs contour value. Note the presence of a singly occupied orbital (SOMO) and a beta LUMO for compound **2**, along with the shape of their isosurfaces, indicative of the asymmetry present in the system.

## Magnetic properties

The paramagnetic properties of **2** were proven by magnetic measurements and EPR spectroscopy. The magnetic susceptibility measurements of compound **2** were carried out on sample **2b** by the Faraday method at 7.3 kOe over the temperature range 300–80–300 K (Figure 8). The data show that there is a hysteresis between magnetic susceptibility values measured upon heating and cooling between 160 and 240 K, where values of magnetic susceptibility in the cooling mode deviate significantly from the Curie-Weiss law. Such behaviour of the sample can be associated with a phase transition. DSC analysis of **2b** shows that there is indeed a second order phase transition at a temperature of 270-300 K (Figure S5). This second-order transition is likely associated with the Jahn-Teller effect described above.

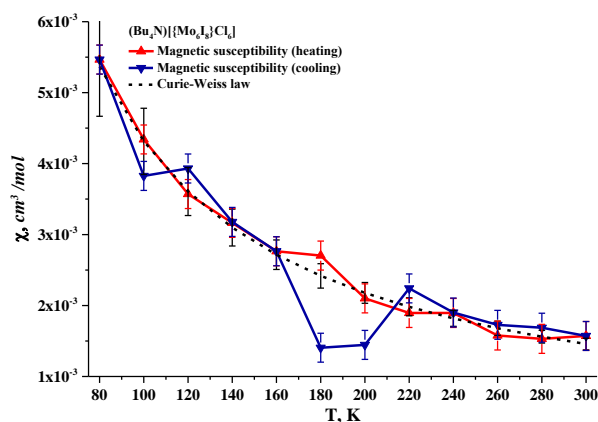


**Figure 8.** Temperature dependence of the magnetic susceptibility for **2b**. Before measurements the sample was kept at the given temperature for at least 10 min.

From the temperature dependence of magnetic susceptibility on the heating mode the constants in the Curie-Weiss dependence:  $\chi = C/(T-\Theta)$  were approximated as  $\Theta = -2(10)$  K and  $C = 0.44(2)$  cm<sup>3</sup> mol<sup>-1</sup> K<sup>-1</sup>. The effective magnetic moment was found to be  $\mu_{eff} = 1.88(5) \mu_B$ , which formally corresponds to  $S = 0.57(5)$  and thus to 1.13  $\bar{e}$  per one cluster anion. This is very close to a theoretical value for one unpaired electron.

The presence of one unpaired electron in the cluster anion was also confirmed by EPR analysis. For this experiment **2b** was directly generated from **1** in the resonator electrochemically by applying a potential of +1.5V. The EPR spectrum of **2b** measured at 300 K (Figure 9) has a single line with half-width  $\Delta H_{1/2} = 5$  mT and  $g$  – factor of 2.01, which is consistent with a 1-electron system in a symmetrical environment and the values of  $g_{\perp}$  and  $g_{\parallel}$  determined for  $[\{\text{Mo}_6\text{Cl}_8\}\text{Cl}_6]^-$  at 10K.<sup>39</sup>

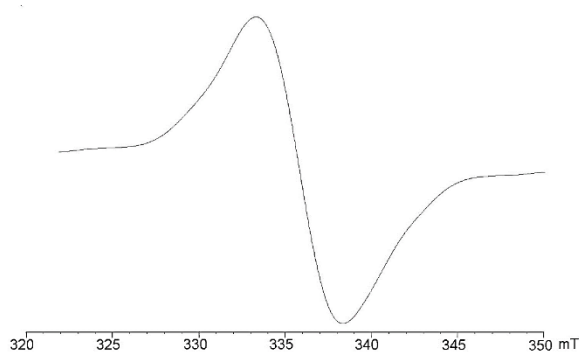


**Figure 9.** EPR spectrum of **2b** at 300K.

### Optical properties of **1** and **2**.

Compound **1** has a typically shaped absorption spectrum for octahedral 24 electron molybdenum compounds with an optical energy gap of about  $\sim 2.1$  eV, which is comparable to those found for  $(\text{Bu}_4\text{N})_2[\{\text{Mo}_6\text{I}_8\}\text{I}_6]$ .<sup>46</sup> One electron oxidation of **1** leads to a striking colour change of the compound from orange into dark-green, which is also confirmed by diffuse reflectance spectroscopy (Figure S6).

As with many other  $24e^-$  octahedral molybdenum cluster compounds, **1** is phosphorescent in the red/near infrared region (Figure S7). Generally the emissive properties of **1** are quite similar to those reported for analogous halide molybdenum cluster complexes, and thus do not require

detailed discussion.<sup>45, 46, 72</sup> However, since the strong effect of both apical (terminal) and inner (cluster core) ligands on the photophysical properties was confirmed by both quantum mechanical calculations<sup>68, 69</sup> and experimentally,<sup>46, 47, 50, 73</sup> it is worth comparing the optical properties of **1** with those of  $(\text{Bu}_4\text{N})_2[\{\text{Mo}_6\text{Cl}_8\}\text{Cl}_6]$  and  $(\text{Bu}_4\text{N})_2[\{\text{Mo}_6\text{I}_8\}\text{Y}_6]$  ( $\text{Y} = \text{Cl}, \text{Br}$  or  $\text{I}$ ). Table 3 summarises known photophysical characteristics - positions of maximum of emission ( $\lambda_{\text{max}}$ ), life times ( $\tau$ ) and photoluminescence quantum yields ( $\Phi$ ) - for these compounds in solid state as well as in deaerated solutions. From the table it is apparent that changing the inner ligand from Cl to I, leads to a hypsochromic shift of the emission maximum and an increase in the life time of emission. This feature is well documented for molybdenum cluster complexes with other types of apical ligands. On the other hand substitution of apical Cl atoms for less electronegative I atoms leads to bathochromic shift of the emission band and some decrease of luminescence quantum yield. This observation is in the agreement with earlier suggestions that the more electron withdrawing the nature of an apical ligand in a molybdenum cluster is, the higher the values of photoluminescence life-times and quantum yields.<sup>22, 45, 46, 50, 73, 74</sup> Overall the photoluminescence of compound **1** in acetone solution gives the highest value recorded for any molybdenum halide cluster complex to date.

**Table 3.** Photophysical characteristics  $\text{A}_2[\{\text{Mo}_6\text{X}_8\}\text{Y}_6]$  in solid state (SS) and in deaerated solutions.

	A	State	$\lambda_{\text{max}} / \text{nm}$	$\Phi$	$\tau / \mu\text{s}$
$\text{A}_2[\{\text{Mo}_6\text{Cl}_8\}\text{Cl}_6]$	$\text{Bu}_4\text{N}$	Acetonitrile <sup>22</sup>	744	0.15	180
$\text{A}_2[\{\text{Mo}_6\text{Br}_8\}\text{Cl}_6]$	Cs	Solid <sup>75</sup>	712	0.21	-
$\text{A}_2[\{\text{Mo}_6\text{I}_8\}\text{Cl}_6]$	$\text{Bu}_4\text{N}$	Solid	704	0.12	6.0 (0.03) 41 (0.19)

					167 (0.78)
		Acetone	707	0.24	154
A <sub>2</sub> [{Mo <sub>6</sub> I <sub>8</sub> }Br <sub>6</sub> ]	Bu <sub>4</sub> N	Solid <sup>76</sup>	710	0.12	-
		Solid <sup>77</sup>	735	0.10	19
A <sub>2</sub> [{Mo <sub>6</sub> I <sub>8</sub> }I <sub>6</sub> ]	Bu <sub>4</sub> N	Acetonitrile <sup>22, 77</sup>	730	0.12	90

---

## CONCLUSION

The cluster complex (Bu<sub>4</sub>N)[{Mo<sub>6</sub>I<sub>8</sub>}Cl<sub>6</sub>] is the first chemically synthesised and isolated as a single phase example of an oxidised molybdenum cluster having a molybdenum halogenide octahedral core {Mo<sub>6</sub>X<sub>8</sub>}<sup>5+</sup>. Importantly, we have demonstrated that [{Mo<sub>6</sub>I<sub>8</sub>}Cl<sub>6</sub>]<sup>-2-</sup> is both a chemically and an electrochemically reversible system. Namely this reversible transition is between a paramagnetic state with one unpaired electron, *i.e.* the 23e<sup>-</sup> [{Mo<sub>6</sub>I<sub>8</sub>}Cl<sub>6</sub>]<sup>-</sup> anion, and a diamagnetic luminescent state - [{Mo<sub>6</sub>I<sub>8</sub>}Cl<sub>6</sub>]<sup>2-</sup>. Due to the high symmetry of the oxidised anion it undergoes dynamic Jahn-Teller D<sub>4h</sub> distortion. Such systems are so far rare but highly attractive not only for applications such as energy-electricity conversion processes and catalysis, but also potentially for use in information storage and random-access memory applications.

## ASSOCIATED CONTENT

**Supporting Information.** The Supporting Information is available free of charge on the ACS Publications website at DOI:

MS, XRPD and DSC data; single crystal data; electrochemical properties; diffuse reflectance spectra; emission spectra. (PDF)

**Accession Codes.** CCDC 1425980, 1576975-1576976, 1588848-1588849 contains the supplementary crystallographic data for this paper. These data can be obtained free of charge via [www.ccdc.cam.ac.uk/data\\_request/cif](http://www.ccdc.cam.ac.uk/data_request/cif), or by emailing [data\\_request@ccdc.cam.ac.uk](mailto:data_request@ccdc.cam.ac.uk), or by contacting The Cambridge Crystallographic Data Centre, 12 Union Road, Cambridge CB2 1EZ, UK; fax: +44 1223 336033.

## **AUTHOR INFORMATION**

### **Corresponding Author**

\*Olga A. Efremova

Tel: +441482465417, Fax: +441482466410

**e-mail:** [o.efremova@hull.ac.uk](mailto:o.efremova@hull.ac.uk)

\*Michael A. Shestopalov

Tel: +73833309253, Fax: +73833309489

**e-mail:** [shtopy@niic.nsc.ru](mailto:shtopy@niic.nsc.ru)

### **Author Contributions**

The manuscript was written through contributions of all authors. All authors have given approval to the final version of the manuscript.

### **Notes**

The authors declare no competing financial interest

## **ACKNOWLEDGMENT**

This work was supported by the Russian Foundation for Basic Research (grant No. 17-03-00140) and by the Grant of the President of the Russian Federation [grant No. MK 180.2017.3]. We

acknowledge the Viper High Performance Computing facility of the University of Hull and its support team. Dr O.A. Efremova thanks EPSRC grant EP/R006393/1. We are grateful to Dr D.G.

Samsonenko (NIIC SB RAS) for collection of X-ray data for compound 1.

## REFERENCES

- (1) Pastore, M., First Principle Modelling of Materials and Processes in Dye-Sensitized Photoanodes for Solar Energy and Solar Fuels. *Computation* **2017**, *5* (1), 5.
- (2) Elgrishi, N.; Chambers, M. B.; Wang, X.; Fontecave, M., Molecular polypyridine-based metal complexes as catalysts for the reduction of CO<sub>2</sub>. *Chem. Soc. Rev.* **2017**, *46* (3), 761-796.
- (3) Windle, C. D.; Perutz, R. N., Advances in molecular photocatalytic and electrocatalytic CO<sub>2</sub> reduction. *Coord. Chem. Rev.* **2012**, *256* (21-22), 2562-2570.
- (4) Thompson, M., The evolution of organometallic complexes in organic light - Emitting devices. *Mrs Bull.* **2007**, *32* (9), 694-701.
- (5) Jou, J. H.; Kumar, S.; Agrawal, A.; Li, T. H.; Sahoo, S., Approaches for fabricating high efficiency organic light emitting diodes. *J. Mater. Chem. C* **2015**, *3* (13), 2974-3002.
- (6) Chi, Y.; Chang, T. K.; Ganesan, P.; Rajakannu, P., Emissive bis-tridentate Ir(III) metal complexes: Tactics, photophysics and applications. *Coord. Chem. Rev.* **2017**, *346*, 91-100.
- (7) Zhao, Y.; Lunt, R. R., Transparent Luminescent Solar Concentrators for Large-Area Solar Windows Enabled by Massive Stokes-Shift Nanocluster Phosphors. *Adv. Energy Mater.* **2013**, *3* (9), 1143-1148.
- (8) Renaud, A.; Grasset, F.; Dierre, B.; Uchikoshi, T.; Ohashi, N.; Takei, T.; Planchat, A.; Cario, L.; Jobic, S.; Odobel, F.; Cordier, S., Inorganic Molybdenum Clusters as Light-Harvester in All Inorganic Solar Cells: A Proof of Concept. *Chemistryselect* **2016**, *1* (10), 2284-2289.
- (9) Barras, A.; Cordier, S.; Boukherroub, R., Fast photocatalytic degradation of rhodamine B over [Mo<sub>6</sub>Br<sub>8</sub>(N<sub>3</sub>)<sub>6</sub>]<sup>2-</sup> cluster units under sun light irradiation. *Appl. Catal. B-Environ.* **2012**, *123*, 1-8.
- (10) Barras, A.; Das, M. R.; Devarapalli, R. R.; Shelke, M. V.; Cordier, S.; Szunerits, S.; Boukherroub, R., One-pot synthesis of gold nanoparticle/molybdenum cluster/graphene oxide nanocomposite and its photocatalytic activity. *Appl. Catal. B-Environ.* **2013**, *130*, 270-276.
- (11) Kumar, P.; Kumar, S.; Cordier, S.; Paofai, S.; Boukherroub, R.; Jain, S. L., Photoreduction of CO<sub>2</sub> to methanol with hexanuclear molybdenum [Mo<sub>6</sub>Br<sub>14</sub>]<sup>2-</sup> cluster units under visible light irradiation. *Rsc Adv.* **2014**, *4* (20), 10420-10423.
- (12) Kumar, P.; Mungse, H. P.; Cordier, S.; Boukherroub, R.; Khatri, O. P.; Jain, S. L., Hexamolybdenum clusters supported on graphene oxide: Visible-light induced photocatalytic reduction of carbon dioxide into methanol. *Carbon* **2015**, *94*, 91-100.
- (13) Kumar, S.; Khatri, O. P.; Cordier, S.; Boukherroub, R.; Jain, S. L., Graphene Oxide Supported Molybdenum Cluster: First Heterogenized Homogeneous Catalyst for the Synthesis of Dimethylcarbonate from CO<sub>2</sub> and Methanol. *Chem. Eur. J.* **2015**, *21* (8), 3488-3494.
- (14) Feliz, M.; Puche, M.; Atienzar, P.; Concepcion, P.; Cordier, S.; Molard, Y., InSitu Generation of Active Molybdenum Octahedral Clusters for Photocatalytic Hydrogen Production from Water. *Chemsuschem* **2016**, *9* (15), 1963-1971.
- (15) Efremova, O. A.; Brylev, K. A.; Vorotnikov, Y. A.; Vejsadova, L.; Shestopalov, M. A.; Chimonides, G. F.; Mikes, P.; Topham, P. D.; Kim, S. J.; Kitamura, N.; Sutherland, A. J.,

Photoluminescent materials based on PMMA and a highly-emissive octahedral molybdenum metal cluster complex. *J. Mater. Chem. C* **2016**, 4 (3), 497-503.

(16) Efremova, O. A.; Brylev, K. A.; Kozlova, O.; White, M. S.; Shestopalov, M. A.; Kitamura, N.; Mironov, Y. V.; Bauer, S.; Sutherland, A. J., Polymerisable octahedral rhenium cluster complexes as precursors for photo/electroluminescent polymers. *J. Mater. Chem. C* **2014**, 2 (40), 8630-8638.

(17) Zheng, Z. P.; Gray, T. G.; Holm, R. H., Synthesis and structures of solvated monoclusters and bridged di- and triclusters based on the cubic building block  $[\text{Re}_6(\mu_3\text{-Se})_8]^{2+}$ . *Inorg. Chem.* **1999**, 38 (21), 4888-4895.

(18) Yoshimura, T.; Umakoshi, K.; Sasaki, Y.; Ishizaka, S.; Kim, H. B.; Kitamura, N., Emission and metal- and ligand-centered-redox characteristics of the hexarhenium(III) clusters trans- and cis- $[\text{Re}_6(\mu_3\text{-S})_8\text{Cl}_4\text{L}_2]_{2-}$ , where L is a pyridine derivative or pyrazine. *Inorg. Chem.* **2000**, 39 (8), 1765-1772.

(19) Adamenko, O. A.; Lukova, G. V.; Golubeva, N. D.; Smirnov, V. A.; Boiko, G. N.; Pomogailo, A. D.; Uflyand, I. E., Synthesis, Structure, and Physicochemical Properties of  $[\text{Mo}_6\text{Cl}_8]^{4+}$ -Containing Clusters. *Dokl. Phys. Chem.* **2001**, 381, 275-278.

(20) Gabriel, J. C. P.; Boubekour, K.; Uriel, S.; Batail, P., Chemistry of hexanuclear rhenium chalcogenide clusters. *Chem. Rev.* **2001**, 101 (7), 2037-2066.

(21) Molard, Y.; Ledneva, A.; Amela-Cortes, M.; Circu, V.; Naumov, N. G.; Meriadec, C.; Artzner, F.; Cordier, S., Ionically Self-Assembled Clustomesogen with Switchable Magnetic/Luminescence Properties Containing  $[\text{Re}_6\text{Se}_8(\text{CN})_6]^{n-}$  (n=3, 4) Anionic Clusters. *Chem. Mater.* **2011**, 23 (23), 5122-5130.

(22) Kirakci, K.; Kubat, P.; Langmaier, J.; Polivka, T.; Fuciman, M.; Fejfarova, K.; Lang, K., A comparative study of the redox and excited state properties of  $(^n\text{Bu}_4\text{N})_2[\text{Mo}_6\text{X}_{14}]$  and  $(^n\text{Bu}_4\text{N})_2[\text{Mo}_6\text{X}_8(\text{CF}_3\text{COO})_6]$  (X = Cl, Br, or I). *Dalton Trans.* **2013**, 42 (19), 7224-7232.

(23) Guilbaud, C.; Deluzet, A.; Domercq, B.; Molinie, P.; Coulon, C.; Boubekour, K.; Batail, P.,  $(\text{NBu}^{4+})_3[\text{Re}_6\text{S}_8\text{Cl}_6]^{3-}$ : synthesis and luminescence of the paramagnetic, open shell member of a hexanuclear chalcogenide cluster redox system. *Chem. Commun.* **1999**, (18), 1867-1868.

(24) Bennett, M. V.; Beauvais, L. G.; Shores, M. P.; Long, J. R., Expanded Prussian blue analogues incorporating  $[\text{Re}_6\text{Se}_8(\text{CN})_6]^{3-/4-}$  clusters: Adjusting porosity via charge balance. *J. Am. Chem. Soc.* **2001**, 123 (33), 8022-8032.

(25) Baudron, S. A.; Deluzet, A.; Boubekour, K.; Batail, P., Jahn-Teller distortion of the open-shell 23-electron chalcogenide rhenium cluster cores in crystals of the series,  $\{[\text{Re}_6\text{Q}_8]^{3+}(\text{X}^-)_6\}^{3-}$  (Q = S, Se; X = Cl, CN). *Chem. Commun.* **2002**, (18), 2124-2125.

(26) Naumov, N. G.; Ostanina, E. V.; Virovets, A. V.; Schmidtman, M.; Muller, A.; Fedorov, V. E., 23-Electron Re-6 metal clusters: Syntheses and crystal structures of  $(\text{Ph}_4\text{P})_3[\text{Re}_6\text{S}_8(\text{CN})_6]$ ,  $(\text{Ph}_4\text{P})_2(\text{H})[\text{Re}_6\text{Se}_8(\text{CN})_6] \cdot 8\text{H}_2\text{O}$ , and  $(\text{Et}_4\text{N})_2(\text{H})[\text{Re}_6\text{Te}_8(\text{CN})_6] \cdot 2\text{H}_2\text{O}$ . *Russ. Chem. Bull.* **2002**, 51 (5), 866-871.

(27) Long, J. R.; McCarty, L. S.; Holm, R. H., A solid-state route to molecular clusters: Access to the solution chemistry of  $[\text{Re}_6\text{Q}_8]^{2+}$  (Q=S, Se) core-containing clusters via dimensional reduction. *J. Am. Chem. Soc.* **1996**, 118 (19), 4603-4616.

(28) Yarovoi, S. S.; Mironov, Y. V.; Naumov, D. Y.; Gatilov, Y. V.; Kozova, S. G.; Kim, S. J.; Fedorov, V. E., Octahedral hexahydroxo rhenium cluster complexes  $[\text{Re}_6\text{Q}_8(\text{OH})_6]^{4-}$  (Q = S, Se): Synthesis, structure, and properties. *Eur. J. Inorg. Chem.* **2005**, (19), 3945-3949.

- (29) Ivanov, A. A.; Kuratieva, N. V.; Shestopalov, M. A.; Mironov, Y. V., Crystal Structure of a  $[\text{CsK}_2(\mu_3\text{-DMF})_2(\mu\text{-DMF})_3(\text{DMF})_4][\{\text{Re}_6(\mu_3\text{-Se})_8\}\text{Br}_6]$  Cluster Complex. *J. Struct. Chem.* **2017**, *58* (5), 989-993.
- (30) Hummel, T.; Strobele, M.; Schmid, D.; Enseling, D.; Justel, T.; Meyer, H. J., Characterization of  $\text{A}_x[\text{W}_6\text{I}_{14}]$  as Key Compounds for Ligand-Substituted  $\text{A}_2[\text{W}_6\text{I}_8\text{L}_6]$  Clusters. *Eur. J. Inorg. Chem.* **2016**, (31), 5063-5067.
- (31) Strobele, M.; Meyer, H. J., The Missing Binary Tungsten Iodide Archetype Cluster  $\text{W}_4\text{I}_{10}$ . *Z. Anorg. Allg. Chem.* **2016**, *642* (24), 1409-1411.
- (32) Schäfer, H.; Siepmann, R., Die Wolframbromide  $\text{W}_6\text{Br}_{12}$ ,  $\text{W}_6\text{Br}_{14}$ ,  $\text{W}_6\text{Br}_{16}$  und  $\text{W}_6\text{Br}_{18}$ . *Z. Anorg. Allg. Chem.* **1968**, *357*, 273-288.
- (33) Siepmann, R.; von Schnerin, H. G., Die Kristallstruktur von  $\text{W}_6\text{Br}_{16}$ . Eine Verbindung mit Polykationen  $[\text{W}_6\text{Br}_8]^{6+}$  und Polyanionen  $[\text{Br}_4]^{2-}$ . *Z. Anorg. Allg. Chem.* **1968**, *357*, 289-298.
- (34) Zietlow, T. C.; Schaefer, W. P.; Sadeghi, B.; Nocera, D. G.; Gray, H. B., Preparation and Properties of bis(triphenylphosphine)iminium tetradecabromohexatungstate. *Inorg. Chem.* **1986**, *25* (13), 2198-2201.
- (35) Saßmannshausen, J.; von Schnerin, H. G., Synthese und Kristallstruktur der molekularen Clusterverbindung  $\text{W}_6\text{Br}_{14}$ . *Z. Anorg. Allg. Chem.* **1994**, *620*, 1312-1320.
- (36) Zheng, Y. Q.; Borrmann, H.; Grin, Y.; Peters, K.; von Schnering, H. G., The cluster compounds  $\text{Ag}[\text{W}_6\text{Br}_{14}]$  and  $\text{Ag}_2[\text{W}_6\text{Br}_{14}]$ . *Z. Anorg. Allg. Chem.* **1999**, *625* (12), 2115-2119.
- (37) Abramov, P. A.; Rogachev, A. V.; Mikhailov, M. A.; Virovets, A. V.; Peresyphkina, E. V.; Sokolov, M. N.; Fedin, V. P., Hexanuclear chloride and bromide tungsten clusters and their derivatives. *Russ. J. Coord. Chem.* **2014**, *40* (5), 259-267.
- (38) Maverick, A. W.; Gray, H. B., Luminescence and Redox Photochemistry of the Molybdenum(II) Cluster  $\text{Mo}_6\text{Cl}_{14}^{2-}$ . *J. Am. Chem. Soc.* **1981**, *103* (5), 1298-1300.
- (39) Maverick, A. W.; Najdzionek, J. S.; Mackenzie, D.; Nocera, D. G.; Gray, H. B., Spectroscopic, Electrochemical, and Photochemical Properties of Molybdenum(II) and Tungsten(II) Halide Clusters. *J. Am. Chem. Soc.* **1983**, *105* (7), 1878-1882.
- (40) Nocera, D. G.; Gray, H. B., Electrochemical Reduction of Molybdenum(II) and Tungsten(II) Halide Cluster Ions - Electrogenerated Chemi-Luminescence of  $\text{Mo}_6\text{Cl}_{14}^{2-}$ . *J. Am. Chem. Soc.* **1984**, *106* (3), 824-825.
- (41) Saito, Y.; Tanaka, H. K.; Sasaki, Y.; Azumi, T., Temperature-Dependence of the Luminescence Lifetime of Hexanuclear Molybdenum(II) Chloride Cluster - Identification of Lower Excited Triplet Sublevels. *J. Phys. Chem.* **1985**, *89* (21), 4413-4415.
- (42) Jackson, J. A.; Turro, C.; Newsham, M. D.; Nocera, D. G., Oxygen Quenching of Electronically Excited Hexanuclear Molybdenum and Tungsten Halide Clusters. *J. Phys. Chem.* **1990**, *94* (11), 4500-4507.
- (43) Kirakci, K.; Cordier, S.; Perrin, C., Synthesis and characterization of  $\text{Cs}_2\text{Mo}_6\text{X}_{14}$  (X= Br or I) hexamolybdenum cluster halides: Efficient Mo-6 cluster precursors for solution chemistry syntheses. *Z. Anorg. Allg. Chem.* **2005**, *631* (2-3), 411-416.
- (44) Ghosh, R. N.; Askeland, P. A.; Kramer, S.; Loloee, R., Optical dissolved oxygen sensor utilizing molybdenum chloride cluster phosphorescence. *Appl. Phys. Lett.* **2011**, *98* (22), 221103.
- (45) Mikhailov, M. A.; Brylev, K. A.; Abramov, P. A.; Sakuda, E.; Akagi, S.; Ito, A.; Kitamura, N.; Sokolov, M. N., Synthetic Tuning of Redox, Spectroscopic, and Photophysical Properties of  $\{\text{Mo}_6\text{I}_8\}^{4+}$  Core Cluster Complexes by Terminal Carboxylate Ligands. *Inorg. Chem.* **2016**, *55* (17), 8437-8445.

- (46) Efremova, O. A.; Vorotnikov, Y. A.; Brylev, K. A.; Vorotnikova, N. A.; Novozhilov, I. N.; Kuratieva, N. V.; Edeleva, M. V.; Benoit, D. M.; Kitamura, N.; Mironov, Y. V.; Shestopalov, M. A.; Sutherland, A. J., Octahedral molybdenum cluster complexes with aromatic sulfonate ligands. *Dalton Trans.* **2016**, *45*, 15427-15435.
- (47) Vorotnikov, Y. A.; Efremova, O. A.; Novozhilov, I. N.; Yanshole, V. V.; Kuratieva, N. V.; Brylev, K. A.; Kitamura, N.; Mironov, Y. V.; Shestopalov, M. A., Hexaazide octahedral molybdenum cluster complexes: Synthesis, properties and the evidence of hydrolysis. *J. Mol. Struct.* **2017**, *1134*, 237-243.
- (48) Evtushok, D. V.; Vorotnikova, N. A.; Logvinenko, V. A.; Smolentsev, A. I.; Brylev, K. A.; Plyusnin, P. E.; Pishchur, D. P.; Kitamura, N.; Mironov, Y. V.; Solovieva, A. O.; Efremova, O. A.; Shestopalov, M. A., Luminescent coordination polymers based on  $\text{Ca}^{2+}$  and octahedral cluster anions  $[\{\text{M}_6\text{Cl}^{18}\}\text{Cl}^{186}\text{]}^{2-}$  (M = Mo, W): synthesis and thermal stability studies. *New J. Chem.* **2017**, *41*, 14855-14861.
- (49) Jackson, J. A.; Mussell, R. D.; Nocera, D. G., Oxidation of Alcohols by Hexanuclear Cluster Ions. *Inorg. Chem.* **1993**, *32* (21), 4643-4645.
- (50) Efremova, O. A.; Shestopalov, M. A.; Chirtsova, N. A.; Smolentsev, A. I.; Mironov, Y. V.; Kitamura, N.; Brylev, K. A.; Sutherland, A. J., A highly emissive inorganic hexamolybdenum cluster complex as a handy precursor for the preparation of new luminescent materials. *Dalton Trans.* **2014**, *43* (16), 6021-6025.
- (51) *CrysAlisPro 1.171.38.41. Rigaku Oxford Diffraction. 2015.*
- (52) Sheldrick, G. M., SHELXT – Integrated space-group and crystalstructure determination. *Acta Cryst.* **2015**, *A71*, 3-8.
- (53) Sheldrick, G. M., Crystal structure refinement with SHELXL. *Acta Cryst.* **2015**, *C71* (3-8).
- (54) Bruker, APEX2 (Version 1.08), SAINT (Version 7.03), SADABS (Version 2.11), SHELXTL (Version 6.12), Bruker AXS Inc., Madison, WI, USA, 2004.
- (55) Becke, A. D., Density-functional thermochemistry. 5. Systematic optimization of exchange-correlation functionals. *J. Chem. Phys.* **1997**, *107* (20), 8554-8560.
- (56) Grimme, S.; Antony, J.; Ehrlich, S.; Krieg, H., A consistent and accurate ab initio parametrization of density functional dispersion correction (DFT-D) for the 94 elements H-Pu. *J. Chem. Phys.* **2010**, *132* (15), 154104.
- (57) Grimme, S.; Ehrlich, S.; Goerigk, L., Effect of the Damping Function in Dispersion Corrected Density Functional Theory. *J. Comput. Chem.* **2011**, *32* (7), 1456-1465.
- (58) Weigend, F.; Ahlrichs, R., Balanced basis sets of split valence, triple zeta valence and quadruple zeta valence quality for H to Rn: Design and assessment of accuracy. *Phys. Chem. Chem. Phys.* **2005**, *7* (18), 3297-3305.
- (59) Weigend, F., Accurate Coulomb-fitting basis sets for H to Rn. *Phys. Chem. Chem. Phys.* **2006**, *8* (9), 1057-1065.
- (60) Neese, F., The ORCA program system. *WIREs Comput. Mol. Sci.* **2012**, *2*, 73-78.
- (61) Neese, F.; Wennmohs, F.; Hansen, A.; Becker, U., Efficient, approximate and parallel Hartree-Fock and hybrid DFT calculations. A 'chain-of-spheres' algorithm for the Hartree-Fock exchange. *Chem. Phys.* **2009**, *356* (1-3), 98-109.
- (62) Vorotnikov, Y. A.; Efremova, O. A.; Vorotnikova, N. A.; Brylev, K. A.; Edeleva, M. V.; Tsygankova, A. R.; Smolentsev, A. I.; Kitamura, N.; Mironov, Y. V.; Shestopalov, M. A., On the synthesis and characterisation of luminescent hybrid particles:  $\text{Mo}_6$  metal cluster complex/ $\text{SiO}_2$ . *Rsc Adv.* **2016**, *6* (49), 43367-43375.

- (63) Vorotnikova, N. A.; Efremova, O. A.; Tsygankova, A. R.; Brylev, K. A.; Edeleva, M. V.; Kurskaya, O. G.; Sutherland, A. J.; Shestopalov, A. M.; Mironov, Y. V.; Shestopalov, M. A., Characterization and cytotoxicity studies of thiol-modified polystyrene microbeads doped with  $[\{\text{Mo}_6\text{X}_8\}(\text{NO}_3)_6]^{2-}$  (X=Cl, Br, I). *Polym. Adv. Technol.* **2016**, *27* (7), 922-928.
- (64) Svezhentseva, E. V.; Solovieva, A. O.; Vorotnikov, Y. A.; Kurskaya, O. G.; Brylev, K. A.; Tsygankova, A. R.; Edeleva, M. V.; Gyrylova, S. N.; Kitamura, N.; Efremova, O. A.; Shestopalov, M. A.; Mironov, Y. V.; Shestopalov, A. M., Water-soluble hybrid materials based on  $\{\text{Mo}_6\text{X}_8\}^{4+}$  (X = Cl, Br, I) cluster complexes and sodium polystyrene sulfonate. *New J. Chem.* **2017**, *41* (4), 1670-1676.
- (65) Madan, R. L., *Organic Chemistry*. Tata McGraw Hill: 2013.
- (66) Bruckner, P.; Preetz, W.; Punjer, M., Synthesis, crystal structure, NMR, vibrational spectra, and normal coordinate analysis of the cluster anions  $[(\text{Mo}_6\text{I}_8^i)\text{Y}_6^a]^{2-}$ ,  $\text{Y}^a=\text{F}, \text{Cl}, \text{Br}, \text{I}$ . *Z. Anorg. Allg. Chem.* **1997**, *623* (1), 8-17.
- (67) Miki, H.; Ikeyama, T.; Sasaki, Y.; Azumi, T., Phosphorescence from the Triplet Spin Sublevels of a Hexanuclear Molybdenum(II) Chloride Cluster Ion,  $[\text{Mo}_6\text{Cl}_{14}]^{2-}$  - Relative Radiative Rate Constants for Emitting Sublevels. *J. Phys. Chem.* **1992**, *96* (8), 3236-3239.
- (68) Ramirez-Tagle, R.; Arratia-Perez, R., Electronic structure and molecular properties of the  $[\text{Mo}_6\text{X}_8\text{L}_6]^{2-}$ ; X = Cl, Br, I; L = F, Cl, Br, I clusters. *Chem. Phys. Lett.* **2008**, *460* (4-6), 438-441.
- (69) Ramirez-Tagle, R.; Arratia-Perez, R., The luminescent  $[\text{Mo}_6\text{X}_8(\text{NCS})_6]^{2-}$  (X = Cl, Br, I) clusters?: A computational study based on time-dependent density functional theory including spin-orbit and solvent-polarity effects. *Chem. Phys. Lett.* **2008**, *455* (1-3), 38-41.
- (70) Deluzet, A.; Duclusaud, H.; Sautet, P.; Borshch, S. A., Electronic structure of diamagnetic and paramagnetic hexanuclear chalcogenide clusters of rhenium. *Inorg. Chem.* **2002**, *41* (9), 2537-2542.
- (71) Gray, T. G., Hexanuclear and higher nuclearity clusters of the Groups 4-7 metals with stabilizing pi-donor ligands. *Coord. Chem. Rev.* **2003**, *243* (1-2), 213-235.
- (72) Kirakci, K.; Fejfarova, K.; Kucerakova, M.; Lang, K., Hexamolybdenum Cluster Complexes with Pyrene and Anthracene Carboxylates: Ultrabright Red Emitters with the Antenna Effect. *Eur. J. Inorg. Chem.* **2014**, 2331-2336.
- (73) Braack, P.; Simsek, M. K.; Preetz, W., Synthesis, crystal structures, and vibrational spectra of  $[(\text{Mo}_6\text{X}_8^i)\text{Y}_6^a]^{2-}$ ;  $\text{X}^i=\text{Cl}, \text{Br}$ ;  $\text{Y}^a=\text{NO}_3, \text{NO}_2$ . *Z. Anorg. Allg. Chem.* **1998**, *624* (3), 375-380.
- (74) Sokolov, M. N.; Mihailov, M. A.; Peresyphkina, E. V.; Brylev, K. A.; Kitamura, N.; Fedin, V. P., Highly luminescent complexes  $[\text{Mo}_6\text{X}_8(\text{n-C}_3\text{F}_7\text{COO})_6]^{2-}$  (X = Br, I). *Dalton Trans.* **2011**, *40* (24), 6375-6377.
- (75) Prévôt, M., *Démonstrateurs des potentialités applicatives des clustomésogènes*. Matériaux: Université Rennes 1, 2014.
- (76) Siva, P., The development of a water-soluble compound containing cluster anion  $[\{\text{Mo}_6\text{I}_8\}\text{F}_6]^{2-}$ . *MChem dissertation University of Hull* **2017**, unpublished.
- (77) Evtushok, D. V.; Melnikov, A. R.; Vorotnikova, N. A.; Vorotnikov, Y. A.; Ryadun, A. A.; Kuratieva, N. V.; Kozyr, K. V.; Obedinskaya, N. R.; Kretov, E. I.; Novozhilov, I. N.; Mironov, Y. V.; Stass, D. V.; Efremova, O. A.; Shestopalov, M. A., A comparative study of optical properties and X-ray induced luminescence of octahedral molybdenum and tungsten cluster complexes. *Dalton Trans.* **2017**, *46*, 11738-11747.

**Either bright or magnetic:** Highly luminescent octahedral cluster anion  $[\{\text{Mo}_6\text{I}_8\}\text{Cl}_6]^{2-}$  oxidises reversibly producing paramagnetic  $[\{\text{Mo}_6\text{I}_8\}\text{Cl}_6]^-$  anion. The properties of the first 23e molybdenum cluster are comprehensively described.

